The Crop Journal 11 (2023) 374–385

Contents lists available at ScienceDirect

The Crop Journal

journal homepage: www.keaipublishing.com/en/journals/the-crop-journal/

BnbHLH92a negatively regulates anthocyanin and proanthocyanidin biosynthesis in *Brassica napus*

Ran Hu [a,b,c,1], Meichen Zhu [a,b,c,1], Si Chen [a,b,c,1], Chengxiang Li [d], Qianwei Zhang [a,b,c], Lei Gao [a,b,c], Xueqin Liu [a,b,c], Shulin Shen [a,b,c], Fuyou Fu [e], Xinfu Xu [a,b,c], Ying Liang [a,b,c], Liezhao Liu [a,b,c], Kun Lu [a,b,c], Hao Yu [d,f], Jiana Li [a,b,c,*], Cunmin Qu [a,b,c,*]

[a] *Chongqing Rapeseed Engineering Research Center, College of Agronomy and Biotechnology, Southwest University, Chongqing 400715, China*
[b] *Academy of Agricultural Sciences, Southwest University, Chongqing 400715, China*
[c] *Engineering Research Center of South Upland Agriculture, Ministry of Education, Chongqing 400715, China*
[d] *Department of Biological Sciences, Faculty of Science, National University of Singapore, Singapore 117558, Singapore*
[e] *Agriculture and Agri-Food Canada, Saskatoon Research Centre, 107 Science Place, Saskatoon, Saskatchewan S7N 02X, Canada*
[f] *Temasek Life Sciences Laboratory, National University of Singapore, Singapore 117604, Singapore*

ARTICLE INFO

Article history:
Received 10 May 2022
Revised 28 June 2022
Accepted 1 August 2022
Available online 24 August 2022

Keywords:
Brassica napus L.
BnbHLH92a
Anthocyanin
Proanthocyanidins
Flavonoid pathway

ABSTRACT

Yellow seed trait is a desirable characteristic with potential for increasing seed quality and commercial value in rapeseed, and anthocyanin and proanthocyanidins (PAs) are major seed-coat pigments. Few transcription factors involved in the regulation of anthocyanin and PAs biosynthesis have been characterized in rapeseed. In this study, we identified a transcription factor gene *BnbHLH92a* (BnaA06T0441000ZS) in rapeseed. Overexpressing *BnbHLH92a* both in *Arabidopsis* and in rapeseed reduced levels of anthocyanin and PAs. Correspondingly, the expression profiles of anthocyanin and PA biosynthesis genes (*TT3*, *BAN*, *TT8*, *TT18*, and *TTG1*) were shown by quantitative real-time PCR to be inhibited in *BnbHLH92a*-overexpressing *Arabidopsis* seeds, indicating that *BnbHLH92a* represses the anthocyanin and PA biosynthesis pathway in *Arabidopsis*. BnbHLH92a physically interacts with the BnTTG1 protein and represses the biosynthesis of anthocyanins and PAs in rapeseed. BnbHLH92a also binds directly to the *BnTT18* promoter and represses its expression. These results suggest that BnbHLH92a is a novel upstream regulator of flavonoid biosynthesis in *B. napus*.

1. Introduction

Rapeseed (*Brassica napus* L., AACC, 2*n* = 38) is one of the most important sources of edible vegetable oil and feed meal, and is also an ideal feedstock for the production of biodiesel [1]. The yellow-seed trait offers several advantages over the black-seed trait: a thinner seed coat, higher oil and protein content, lower cellulose and polyphenolic contents, and clearer oil [2]. Breeders are attempting to develop yellow-seeded rapeseed for further improving the quality of rapeseed meal and oil [3–6].

Natural rapeseed germplasm with the yellow-seeded trait has not been found. Seed coat color is a quantitative trait affected by multiple factors, including polygenic control, maternal effects, and environment [2,7–9]. For this reason, molecular genetic mechanisms controlling the yellow-seeded trait are not well understood. Proanthocyanidins (PAs, known as condensed tannins) are the main flavonoids that affect seed coat color in *Brassica* species [10–12], and are formed from anthocyanidin as a precursor, sharing the same upstream pathway with anthocyanins in branches of the flavonoid pathway [13]. In *Arabidopsis thaliana*, however, formation of seed color involves the flavonoid pathway, which has also been well characterized in *transparent testa* (*TT*) mutants, including mutants of more than 21 *TT*-type genes (such as *tt1–tt19*, *Transparent Testa Glabra 1* (*ttg1*), and *Transparent Testa Glabra 2* (*ttg2*)) [14–16]. Most of these genes have also been identified and associated with the flavonoid biosynthesis pathway in various *Brassica* species, such as *TTG1* in *B. rapa* [17]; *TT8* in *B. rapa* [18], *B. juncea* [19], and *B. napus* [20]; and *BnTT1* in *B. napus* [21]. These genes display expression patterns that differ between black- and yellow-seeded *Brassica* lines [22–26].

* Corresponding authors.
E-mail addresses: ljn1950@swu.edu.cn (J. Li), drqucunmin@swu.edu.cn (C. Qu).
[1] These authors contributed equally to this work.

https://doi.org/10.1016/j.cj.2022.07.015

In most plants, the ternary MYB–bHLH–WDR (MBW) complex functions in the flavonoid biosynthesis pathway by regulating the expression levels and patterns of the structural genes [27–29]. Among them, TT2 (R2R3-MYB), TT8 (basic helix-loop-helix, bHLH), and WD40 transcription factors form ternary MYB–bHLH–WDR (MBW) complexes, which influence the flavonoid biosynthesis pathway by regulating the expression levels and patterns of the underlying structural genes in developing seeds, including *Dihydroflavonol-4-reductase* (*DFR*), *Leucoanthocyanidin Dioxygenase* (*LDOX*/*TT18*), *Banyuls* (*BAN*), *Glutathione S-transferase 26* (*GST26*/*TT19*), and MATE transporter *TT12*, leading to changes in the color of seed coat [15,27–29]. Three MBW complexes (MYB5–TT8–TTG1, TT2–EGL3–TTG1, and TT2–GL3–TTG1) have also been shown [30] to function in a tissue-specific manner. Transient expression of *DkMYB2*, *DkMYB4*, and *DkMYC1* synergistically increased the expression of *ANTHOCYANIN REDUCTASE* (*ANR*) in persimmon (*Diospyros kaki*) fruit, thereby regulating the accumulation of PAs [31]. A complex, AN2–AN1–AN11, consisting of the MYB protein ANTHOCYANIN2 (AN2), bHLH protein AN1, and WD40 protein AN11, is required for anthocyanin synthesis and acidification of the vacuole in petals of *Petunia hybrida* [32–34]; and MYBA–bHLH3–TTG1 regulates anthocyanin biosynthesis. In mulberry fruits, TT2L1 and TT2L2 work with bHLH3 or GL3 and form an MBW complex with TTG1 to regulate PA biosynthesis [35]. Although considerable information is available about the roles of MBW complexes in governing the flavonoid biosynthesis pathway in many species, little is known about the regulation of MBW complexes in allotetraploid rapeseed.

In the MBW complex model, bHLH is considered [36] a conserved core component that serves as a bridge between MYB and WD40. Studies of transcription factors that affect anthocyanin/PAs biosynthesis have focused mainly on MYBs, including MYB11, MYB12, and MYB111, which regulate the expression of the early anthocyanin and PA biosynthetic genes *CHS*, *CHI*, and *F3H* [37–39], and AtMYB75/PAP1, AtMYB90/PAP2, MYB113, MYB114, and TT2 (*AtMYB123*), which regulate the expression of late anthocyanin and PA biosynthetic genes [28,39–43]. bHLH transcription factors can affect the binding affinity of MYB to a *cis* element of a target gene [27,44]. GL3, EGL3, and TT8 interact with R2R3-MYB proteins and are involved in the regulation of flavonoid biosynthesis in *A. thaliana* [28,40,45]. Recently, some mechanisms by which bHLHs participate in flavonoid metabolic regulation have also been revealed in other plants. LcbHLH92 is a negative regulator of the anthocyanin and PA pathway in sheepgrass (*Leymus chinensis*) that influences seed dormancy, primarily by increasing the transcript levels of *jasmonate-ZIM* (*JAZ*) genes to repress the anthocyanin and PA pathway [46]. The *Chimonanthus praecox* gene *CpbHLH1* is the first anthocyanin biosynthesis inhibitor gene identified in dicots [36]. Overexpressing *VdbHLH037* from spine grape (*Vitis davidii*) promotes anthocyanin accumulation in *A. thaliana* by regulating the expression of genes (*CHI*, *CHS*, *F3H*, *DFR*, *LDOX*, and *UGT78D2*) in the anthocyanin biosynthesis pathway [47]. However, the functional roles of numerous bHLH transcription factors in *B. napus* remain largely unknown.

In investigating the yellow-seed trait in rapeseed, we found by transcriptome analysis (Fig. S1) that the *bHLH* transcription factor gene, *BnbHLH92a* (BnaA06T0441000ZS), was differentially expressed between yellow- and black-seeded rapeseeds at various seed developing stages. The object of the present study was to isolate *BnbHLH92a* from rapeseed, and overexpress *BnbHLH92a* to identify their biological functions and biotechnological potential by transforming *Arabidopsis thaliana* and rapeseed. Our findings shed light on the transcriptional regulation of the flavonoid biosynthesis pathway in *Brassica* plants.

2. Materials and methods

2.1. Plant materials and growth conditions

The rapeseed cultivars ZY821 (black-seeded) and GH06 (yellow-seeded) were grown under field conditions in three rows at each site (0.4 m between rows and 0.2 m between plants) in the experimental field in Beibei (106.38°E, 29.84°N), Chongqing, China. To investigate the expression profiles of *BnbHLH92a* during seed maturation, the flowers were marked with different colors of wool to identify seeds at the same development stages. At 7, 21, 28, and 42 days after flowering (d), immature seeds were gently harvested from siliques, frozen in liquid nitrogen, and then held at –80 °C for total RNA extraction.

The wild-type *A. thaliana* (ecotype Col-0) and transgenic plants were grown in an illumination incubator at 22 °C/16 h in the light, followed by 18 °C/8 h in the dark, with a light level of 12,000 lx and relative humidity of approximately 80%. As with *B. napus*, seeds harvested from siliques at 10 D were used for further analysis. Wild-type *Nicotiana benthamiana* plants were grown in an incubator under long-day conditions (16-h-light/8-h-dark photoperiod) with 10,000 lx supplementary light at room temperature (25 °C).

2.2. Gene cloning, phylogenetic analysis, and expression analysis

Total RNA was extracted from *B. napus* using a DNA Away RNA Mini-Prep Kit (Sangon Biotech, Shanghai, China) following the manufacturer's instructions. Full-length *BnbHLH92a* cDNA was amplified with gene-specific primers (Table S1). The protein sequences of gene homologs were retrieved from the NCBI database (http://www.ncbi.nlm.nih.gov/) and the BnPIR (*Brassica napus* pan-genome information resource, http://cbi.hzau.edu.cn/bnapus/index.php). Multiple sequence alignment was performed with COBALT (Constraint-based Multiple Alignment Tool; https://www.ncbi.nlm.nih.gov/), and a phylogenetic tree was constructed using MEGA7 (Lynnon Biosoft, Quebec, Canada) by the neighbor-joining method [48]. Transcriptome data of *BnbHLH92a* in tissues and organs of *B. napus* from the BrassicaEDB database (https://brassica.biodb.org/) [49]. qRT-PCR was performed on a CFX96 real-time PCR machine (Bio-Rad Laboratories, Hercules, CA, USA) using AceQ Universal SYBR qPCR Master Mix (Vazyme Biotech, Nanjing, Jiangsu, China). The internal reference genes used were *BnACTIN7* in *B. napus* and *AtActin2* in *A. thaliana*. Reactions were performed with three biological and three technical replicates per sample. Relative gene expression levels were calculated by the $2^{-\Delta\Delta CT}$ method [50]. All gene-specific primers are listed in Table S1.

2.3. Transformation of BnbHLH92a in Arabidopsis and B. Napus

The open reading frame (ORF) of *BnbHLH92a* was amplified with specific primers (Table S1) and cloned into the pEarlyGate101 binary vector [51] with C-terminal fusion with EYFP under the control of the 35S promoter. The recombinant destination plasmid pEarlyGate101::*BnbHLH92a*-EYFP (Fig. S2A) was transformed into *Agrobacterium tumefaciens* GV3101 by chemical transformation and transformed into *A. thaliana* (Col-0) and *B. napus* using the floral dip method and *Agrobacterium tumefaciens*-mediated hypocotyl transformation as previously described [38,52,53]. Transgenic plants were preliminarily screened using 1 mL^{-1} of 10% Basta solution, and the transgenic status of surviving plants was further confirmed by PCR analysis. The primer sequences are listed in Table S1.

2.4. Subcellular localization of BnbHLH92a

To express *BnbHLH92a* in *N. benthamiana* epidermal cells, the ORF of *BnbHLH92a* was cloned into pNC-Cam1304-SubN harboring

the *GFP* sequence to generate an N-terminal fusion with GFP [54], resulting in the Pro35S-*BnbHLH92a:GFP* fusion vector (Fig. S2B). The recombinant plasmid Pro35S-*BnbHLH92a:GFP* and the control plasmid pNC-Cam1304-SubN were transformed into *A. tumefaciens* strain GV3101 (with the pSoup helper plasmid), and were also injected into leaf epidermal cells of 6- to 8-week-old *N. benthamiana* plants, as previously described [43]. The epidermal cells were stained with DAPI and fluorescent signals were observed under a confocal laser-scanning microscope (LSM802400301, Carl Zeiss, Oberkochen, Germany) two days after infiltration.

2.5. In situ hybridization

Seeds from a pair of yellow- and black-seeded plant lines at 21 D were selected as the experimental materials. *In situ* hybridization was performed as previously described [55,56]. Seeds were harvested and fixed overnight in formaldehyde alcohol acetic acid (FAA) (Coolaber, Beijing, China). The samples were dehydrated in a graded ethanol series and embedded in paraffin. Longitudinal sections (8 μm thick) were prepared from the seeds using an RM2235 rotary microtome (Leica Microsystems, Wetzlar, Germany). A 193-bp fragment of *BnbHLH92a* cDNA was used as a probe sequence (5′-ACATATGATGAAAGAGAGAACGAGAAGAGA GAAACAAAAACAGAGTTACTTAGCTCTCCAATCTCTATTACCATTTGCC ACTAAGAATGACAAAAATTCGATTGTTGAAAAGGCCGTTGATCAGATT AGGAAATTAGACGAATATAAGAAAGAACTAGAGAGAAAAATGAATG TGTTGGAGGCAAAATCAGCA-3′), which was amplified by RT-PCR using PrimeScript (TaKaRa Bio, Inc., Dalian, Liaoning, China) and cloned into the pGEM-T Easy vector (Promega). Sense and antisense probes were generated using a PCR DIG Probe Synthesis Kit (Roche Applied Science). Hybridization and detection were performed according to the Nonradioactive In Situ Hybridization Application Manual (Roche Applied Science).

2.6. Yeast two-hybrid analysis

To identify proteins that might interact with BnbHLH92a, yeast two-hybrid (Y2H) assays were performed using the Matchmaker Gold Y2H System (Clontech, USA). The full-length coding sequence of *BnbHLH92a* was cloned into the pGBKT7 (binding domain, BD) vector (Fig. S2C). The full-length coding sequences of *BnTTG1a* (BnaA06T0329200ZS) and *BnTTG1b* (BnaC07T0364700ZS) were each ligated into the pGADT7 (activation domain, AD) vector (Fig. S2D and E). The AD and BD fusion vectors were introduced into yeast (*Saccharomyces cerevisiae*) strain Y2HGold using the polyethylene glycol/lithium acetate method described in the Yeast Protocol Handbook (Clontech). Co-transformed colonies were initially grown separately on SD/-Trp/-Leu plates and further screened for growth on SD/-Trp/-Leu/-His/-Ade plates. The pGADT7-T and pGBKT7-53 vectors were used as a positive control. All experiments were repeated three times. The primers used in this experiment are listed in Table S1.

2.7. Bimolecular fluorescence complementation (BiFC) assays

The ORFs of *BnTTG1a*, and *BnTTG1b* were amplified and separately inserted into pNC-Cam1304-SubN [54] to generate N-terminal fusion proteins with GFP (Fig. S2F and G). To detect genetic interactions, the full-length CDS of *BnbHLH92a* was cloned into the pNC-BiFC-Ecc vector [54] to fuse with the C-terminal fragment of YFP (cYFP) (Fig. S2H), and *BnTTG1a* and *BnTTG1b* were individually cloned into the pNC-BiFC-Enn vector [54] to generate *BnTTG1a*/*BnTTG1b*-nYFP plasmids (Fig. S2I and J). The plasmids were transformed into *A. tumefaciens* strain GV3101 (with the pSoup helper plasmid). *A. tumefaciens* cultures harboring different combinations of BiFC vectors were resuspended in infiltration buffer (10 mmol L^{-1} MES, 10 mmol L^{-1} $MgCl_2$, and 0.15 mmol L^{-1} acetosyringone) and injected into the epidermal cells of 6- to 8-week-old *N. benthamiana* plants as described [43]. Transfected cells were imaged under the confocal laser-scanning microscope and the positions of nuclei were confirmed by DAPI DNA staining. The primers used in the experiment are listed in Table S1.

2.8. Transient dual-luciferase expression assays

To investigate the transcriptional repressor activity of BnbHLH92a, the VP16 vector harboring the coding region of *BnbHLH92a* and the empty VP16 vector were used as effectors. The reporter vector contained five copies of the GAL4 binding element and the minimal CaMV 35S promoter fused to the firefly luciferase (*LUC*) reporter gene, whereas the Renilla luciferase (*REN*) reporter gene under the control of the 35S promoter was used as an internal control. The primers used in the experiment are listed in Table S1.

To assay the binding of BnbHLH92a to the *BnTT18* promoter, the promoter sequence of *BnTT18* was cloned into the pNC-Green-LUC vector [54] to generate the luciferase reporter gene (*BnTT18pro*-LUC; Fig. S2K). *BnbHLH92a* was cloned into the pNC-Green-SK vector [54] to generate the effector construct (35Spro::*BnbHLH92a*; Fig. S2L). *Arabidopsis* protoplasts were transformed with the effector and reporter constructs with an *Arabidopsis* Protoplast Preparation and Transformation Kit (Coolaber). The LUC/REN ratio was determined using the Dual-Glo Luciferase Assay System (Promega) on a luminescence detector (Promega, GloMax 20/20) after 12–16 h to identify transcriptional regulation. At least six biological replicates were conducted for each combination. The primers used in the experiment are listed in Table S1.

2.9. Chromatin immunoprecipitation quantitative PCR (ChIP-qPCR) assay

ChIP was performed according to the protocols in ChIP Assay Kit (Beyotime, Shanghai, China). Seeds of *OE-BnbHLH92a* rapeseed were placed in crosslink buffer containing 1% formaldehyde for vacuum crosslinking for 15 min, and 100 mmol L^{-1} glycine was added for 5 min to stop crosslinking. The chromatin was fragmented by sonication, with fragments concentrated mainly at 100–200 bp. The protein-DNA complex was captured by anti-GFP antibody, with rabbit IgG was used as a mock antibody for negative control. Finally, immunoprecipitated chromatin was subjected to real-time qPCR using AceQ Universal SYBR qPCR Master Mix (Vazyme).

2.10. Histochemical staining of PAs

Mature seeds were harvested from wild-type and *BnbHLH92a*-overexpressing T_4 plants and stained with 0.3% (w/v) 4-dimethylaminocinnamaldehyde (DMACA) solution as described previously [57]. The samples were incubated for ~1 h at room temperature and rinsed several times with 70% (v/v) ethanol. Digital images were acquired under an Olympus SZX7 stereomicroscope (Olympus, Tokyo, Japan) and processed with Adobe Photoshop CS6.0 software (Adobe, San Jose, USA).

2.11. Metabolite measurements

Anthocyanins were isolated from seeds with extraction solution (0.1% HCl in methanol), and the absorption of the extracts was measured at 535 nm with an ultraviolet spectrophotometer (UH5300 UV/VIS, Tokyo, Japan). Anthocyanin levels are reported as $10 \times (A_{535})\ g^{-1}$ fresh weight (FW) [58]. Soluble and insoluble PA contents were determined using a heated butanol/HCl method at 550 nm as previously described [59,60]. PA levels (soluble and insoluble) were represented by $(A_{550})\ g^{-1}$ FW. At least three biological replications were performed.

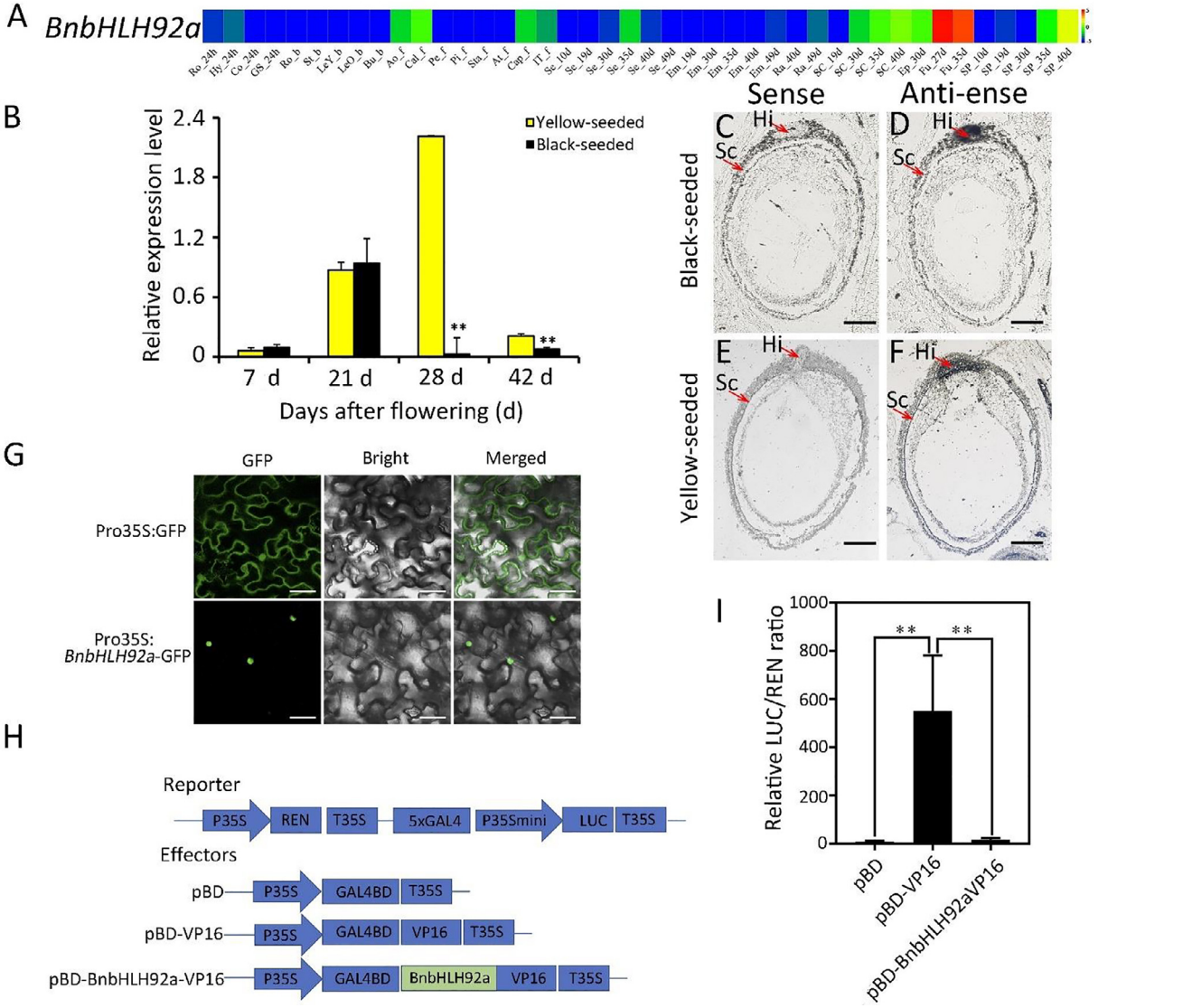

Fig. 1. Characterization of BnbHLH92a. (A) Expression patterns of *BnbHLH92a* in tissues and organs of *B. napus*. Ro, roots; Hy, hypocotyl; Co, cotyledon; GS-24 h, 24 h after seed germination; St, stems; LeY, young leaves; LeO, old leaves; Bu, buds; Ao, anthocaulus; Cal, calyx; Pe, petals; Pi, pistil; Sta, stamen; At, anthers; Cap, capillaments; IT, inflorescence tip; f, flowering stage; Se, seeds; Em, embryo; Ra, radicle apices; SC, seed coat; Ep, episperm; Fu, funicles; SP, silique pericarp; numbers and the letter d indicate days after flowering. Bar represents the $\log_2$ expression level (FPKM). (B) Expression patterns of *BnbHLH92a* in the seed coats of yellow- and black-seeded rapeseed revealed by qRT-PCR analysis. Values are mean ± SD of three technical replicates (**, $P < 0.01$). d, days after flowering. (C–F) *In situ* hybridization of *BnbHLH92a* in yellow- and black-seeded *B. napus* seed. (C, E) *In situ* hybridization of *BnbHLH92a* in yellow- and black-seeded *B. napus* seed using sense probe. (D, F) *In situ* hybridization of *BnbHLH92a* in yellow- and black-seeded *B. napus* seeds using antisense probe. Longitudinal sections at 20 d. SC, seed coat; Hi, hilum. Scale bars, 100 μm. (G) BnbHLH92a is localized to the nucleus in *N. benthamiana* leaf epidermal cells. *BnbHLH92a*-GFP or GFP was transiently expressed in *N. benthamiana* leaf epidermal cells. Scale bars, 50 μm. (H) Schematic diagram of the double-reporter and effector plasmids used in the dual-luciferase assay. (I) Transcriptional repression ability of BnbHLH92a protein in *Arabidopsis* protoplasts. Values are mean ± SD of three technical replicates (**, $P < 0.01$).

To measure the primary phenolic and flavonoid components, fresh seeds (100 mg) were quickly crushed into powder and homogenized in an aqueous solution of formic acid (0.1% [v/v]) in aqueous methanol (1 mL; 80% [v/v]). The sample was then sonicated (KQ-100E, Kunshan, China) for 1 h, and the crude extracts were centrifuged for 15 min at 10,000×*g*. Finally, the supernatant was filtered through a 0.22-μm nylon filter, and phenolic and flavonoid contents were measured by UPLC-HESI-MS/MS as described previously [61]. All samples were assayed in three replicates.

2.12. Statistical analysis

To ensure reliability and reproducibility, all experiments were performed at least three times. Significance of differences was tested by Student's *t*-test. Principal component analysis (PCA) was performed on the web-based sever Metabolite Sets Enrichment Analysis 4.0 (MSEA 4.0 or MetaboAnalyst 4.0; https://www.metaboanalyst.ca, accessed on March 22, 2020).

2.13. Accession numbers

The GenBank accession numbers of the bHLH gene sequences are as follows: *AtbHLH92* (NP_199178.1), *LcbHLH92a* (KY000709.1), *LcbHLH92b* (KY000710.1), *PobHLH92* (XP_034930892.1), *CsbHLH91* (XP_030497714.1), *BobHLH92* (Bol027107), *BrbHLH92* (Bra033690), *ZmbHLH92* (XP_008656601.1), *OsbHLH92* (Os03g53020.1), *MdMYC2* (NP_001315873.1), *ZmbHLLH87* (XP_008656601.1), *GlybHLH92* (XP_028191547.1), *SolbHLH92* (Solyc09g083360.2.1), *OsbHLH68*

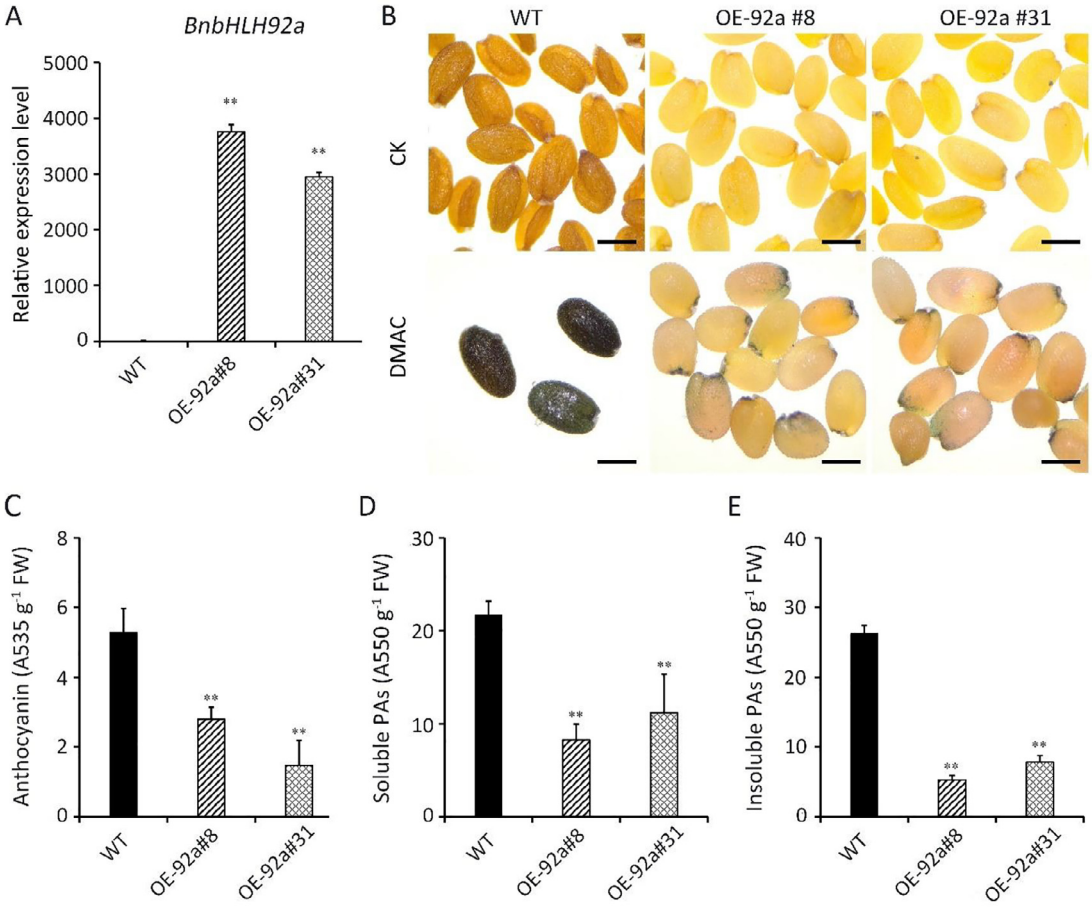

Fig. 2. BnbHLH92a negatively regulates anthocyanin and PA accumulation in *A. thaliana*. (A) Relative expression levels of *BnbHLH92a* in OE-92a *A. thaliana* lines. The *A. thaliana ACTIN* gene was used as an internal control. (B) DMACA staining of OE-92a and wild-type control seeds. WT, wild type; CK, control; DMACA, 4-dimethylaminocinnamaldehyde. Scale bars, 1 μm. (C) Anthocyanin levels in WT and two transgenic lines. (D) Soluble PA levels in WT and two transgenic lines. (E) Insoluble PA levels in WT and two transgenic lines. Values are mean ± SD of three biological replicates (**, $P < 0.01$).

(XP_025879889.1), *AtTT8* (NP_192720), *PpbHLH10* (XP_020413511.1), *AtbHLH3* (AT4G16430), *BnbHLH112* (XP_013687232.1), and *AtbHLH13* (AT1G01260).

3. Results

3.1. BnbHLH92a is a candidate regulator for yellow-seeded B. Napus

In *B. napus*, 602 potential bHLHs were categorized into 35 subfamilies [62]. Among them, BnbHLH92, which could be a G-box binding protein, was grouped into the S7 subfamily. BnbHLH92a contained a basic helix-loop-helix domain (Fig. S3A). In the phylogenetic tree, BnbHLH92a and AtbHLH92 clustered with LcbHLH92 (Fig. S3B), a negative regulator involved in the anthocyanin and PA pathway in sheepgrass [46].

BnbHLH92a is expressed predominantly in the seed (35 after days pollination, Se_35d), seed coat (30, 35 and 40 after days pollination, SC_30d, SC_35d, and SC_40d), episperm (30 after days pollination, Ep_30d), funicle (27 and 35 after days pollination, Fu_27d and Fu_35d), and silique pod (35 and 40 after days pollination, SP_35d and SP_40d) (Fig. 1A). The full-length cDNA of *BnbHLH92a* (BnaA06T0441000ZS) spanned 717 bp (Table S2), encoding a 238-amino-acid protein with a predicted molecular weight of 27.58 kDa and a calculated isoelectric point of 10.0. Transcripts of *BnbHLH92a* in developing seeds were found at higher levels in the seed coats of yellow-seeded than of black-seeded lines (Figs. 1B, S1). These transcripts were detected by *in situ* hybridization in the seed coat and hilum of yellow- but not black-seeded lines (Fig. 1C–F).

3.2. BnbHLH92a is localized to the nucleus and acts as a repressor

The control GFP protein produced fluorescence signals in both the cytoplasm and nucleus, whereas the Pro35S:BnbHLH92a-GFP fusion protein was detected exclusively in the nucleus (Fig. 1G), indicating that BnbHLH92a acts as a transcription factor.

To investigate whether BnbHLH92a is a transcriptional activator or repressor, the open reading frame sequence of *BnbHLH92a* was inserted into the pBD-VP16 vector as effector, and a construct encoding the VP16 transcriptional activation domain was used as a positive control (Fig. 1H). Protoplasts carrying pBD-BnbHLH92a-VP16 showed lower expression of the *LUC* reporter than those carrying pBD-VP16 (Fig. 1I), suggesting that BnbHLH92a functions as a transcriptional repressor.

3.3. Overexpression of BnbHLH92a inhibits anthocyanin and PAs biosynthesis in transgenic Arabidopsis

To identify the biological function of BnbHLH92a, we constructed an overexpression vector harboring *BnbHLH92a* driven by the 35S promoter and used it to transform wild-type *A. thaliana* by *A. tumefaciens*-mediated transformation. We generated 10 independently transformed lines with marked phenotypic variation in seed coat

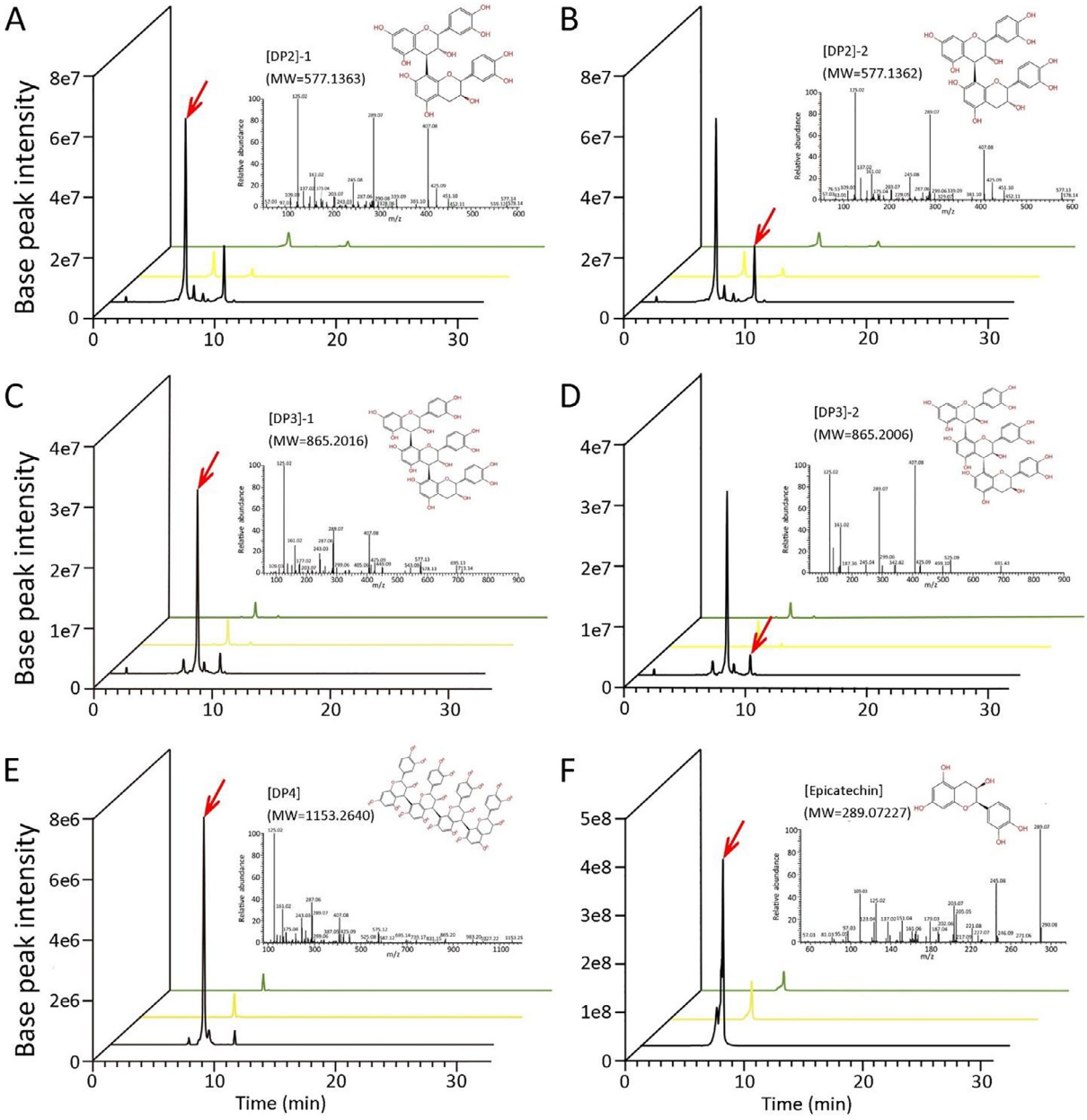

Fig. 3. UPLC-HESI-MS/MS chromatograms of constituents detected in seeds of wild type and *OE-92a Arabidopsis* plants. (A) [DP2]-1. (B) [DP2]-2. (C) [DP3]-1. (D) [DP3]-2. (E) [DP4]. (F) Epicatechin. The black, yellow, and green lines indicate WT, OE-92a #8, and OE-92a #31, respectively.

Table 1
Flavonoids with significantly different abundances identified by UPLC-HESI-MS/MS in seed extracts of wild-type vs. OE-92a *Arabidopsis* (μg g^{-1} FW).

Compound name	WT	OE-92a #8	OE-92a #31
[DP2]-1	1.3312 ± 0.4033	0.0968 ± 0.0104**	0.0653 ± 0.005**
[DP2]-2	0.3739 ± 0.0785	0.0284 ± 0.0021**	0.0200 ± 0.0002**
[DP3]-1	0.5965 ± 0.1492	0.0436 ± 0.0048**	0.0287 ± 0.0026**
[DP3]-2	0.0648 ± 0.0158	0.0045 ± 0.0009**	0.0031 ± 0.0002**
[DP4]	0.1365 ± 0.0425	0.0073 ± 0.0011**	0.0052 ± 0.0006**
Epicatechin	10.2335 ± 1.7408	1.0090 ± 0.2294**	0.6633 ± 0.0274**

Values are mean ± SD of three independent experiments. **, $P < 0.01$.

color (Fig. S4). Two independent lines (OE-92a #8 and OE-92a #31) were confirmed by qRT-PCR and selected for additional analysis. *BnbHLH92a* was strongly upregulated in both lines (Fig. 2A) with the yellow seed coat color (Fig. 2B). Two studies [30,63] have shown that PAs are metabolites determining seed coat color in *A. thaliana*. Histochemical staining with DMACA revealed obviously decreases in PA levels in the *OE-92a* lines relative to the wild-type control (Fig. 2B). Correspondingly, a significant reduction in the contents of anthocyanin (Fig. 2C) and PAs (soluble and insoluble) was detected in the *BnbHLH92a-OE* lines relative to WT (Fig. 2D–E).

To investigate in detail the role of BnbHLH92a in the flavonoid biosynthesis pathway, we quantified the primary phenolic and flavonoid components in the transgenic lines by ultra-high-pressure liquid chromatography with heated electrospray ionization tandem mass spectrometry (UPLC-HESI-MS/MS; Fig. S5; Table S3). The contents of individual flavonoids and their metabolic derivatives differed between *OE-92a* and WT plants, especially epicatechin and PAs (Fig. 3; Table 1), suggesting that BnbHLH92a functions in regulating anthocyanin and PAs accumulation.

As expected, the flavonoid biosynthetic genes, including *AtTT3*, *AtTT18*, *AtBAN*, *AtTT8*, and *AtTTG1*, were significantly inhibited after overexpression of *BnbHLH92a*, in agreement with the reduction of phenolic and flavonoid levels in the *OE-92a* lines compared to WT (Fig. 4A). These findings indicate that BnbHLH92a negatively regulates flavonoid biosynthesis in *OE-92a* plants. However, study has shown that JASMONATE-ZIM-domain (JAZ) genes interact directly with bHLH (TT8, GL3, EGL3) and R2R3-MYB (MYB75) in the MBW complex, and inhibit the accumulation of anthocyanins regulated by jasmonate [64]. In our study, the expression levels of JASMONATE-ZIM-domain (JAZ) genes, including *AtJAZ5*, *AtJAZ6*, *AtJAZ8*, and *AtJAZ10*, were much higher in the *OE-92a* lines than in the WT (Fig. 4B). These results are in agreement with a previous finding that bHLH92 inhibits the expression of *TT8* by activating *JAZ* gene expression in sheepgrass [46]. The expression level of *AtTTG1* was also significantly reduced in the *OE-92a* lines (Fig. 4A), suggesting that BnbHLH92a negatively regulated flavonoid biosynthesis in *A. thaliana* by directly interacting with TTG1, and BnbHLH92a functions as a transcriptional repressor to regulate the anthocyanin and PA accumulation that determines the seed color of *A. thaliana* (Fig. 4C).

3.4. BnbHLH92a affects the accumulation of anthocyanin and PA accumulation in rapeseed

Although *Arabidopsis* and *B. napus* have a close evolutionary relationship, rapeseed, as an allotetraploid, has a more complex genome than *Arabidopsis*. *OE-BnbHLH92a* lines and ZS11 could be divided into two groups with significant differences according to a principal component analysis (PCA) of the content of internal metabolites (Fig. 5A). Compared with the control (ZS11), a variety of differentially abundant metabolites were identified in *OE-BnbHLH92a* lines, including flavone and flavonol, anthocyanins, and PAs and their derivatives (Fig. 5B). Among them, procyanidin B2 ([DP2]-1) and [DP2]-2, procyanidin C ([DP3]-1) and [DP3]-2, [DP4], and epicatechin were significantly reduced in the *OE-BnbHLH92a* lines (Fig. 5C–H), a finding consistent with the finding of differential abundance of flavonoid metabolites in the transgenic *Arabidopsis*, suggesting that *BnbHLH92a* could negatively regulate anthocyanin and PA accumulation in *B. napus*.

3.5. BnbHLH92a interacts physically with BnTTG1

The MBW protein complex influences the expression of structural genes in the flavonoid pathway [27–29]. In this study,

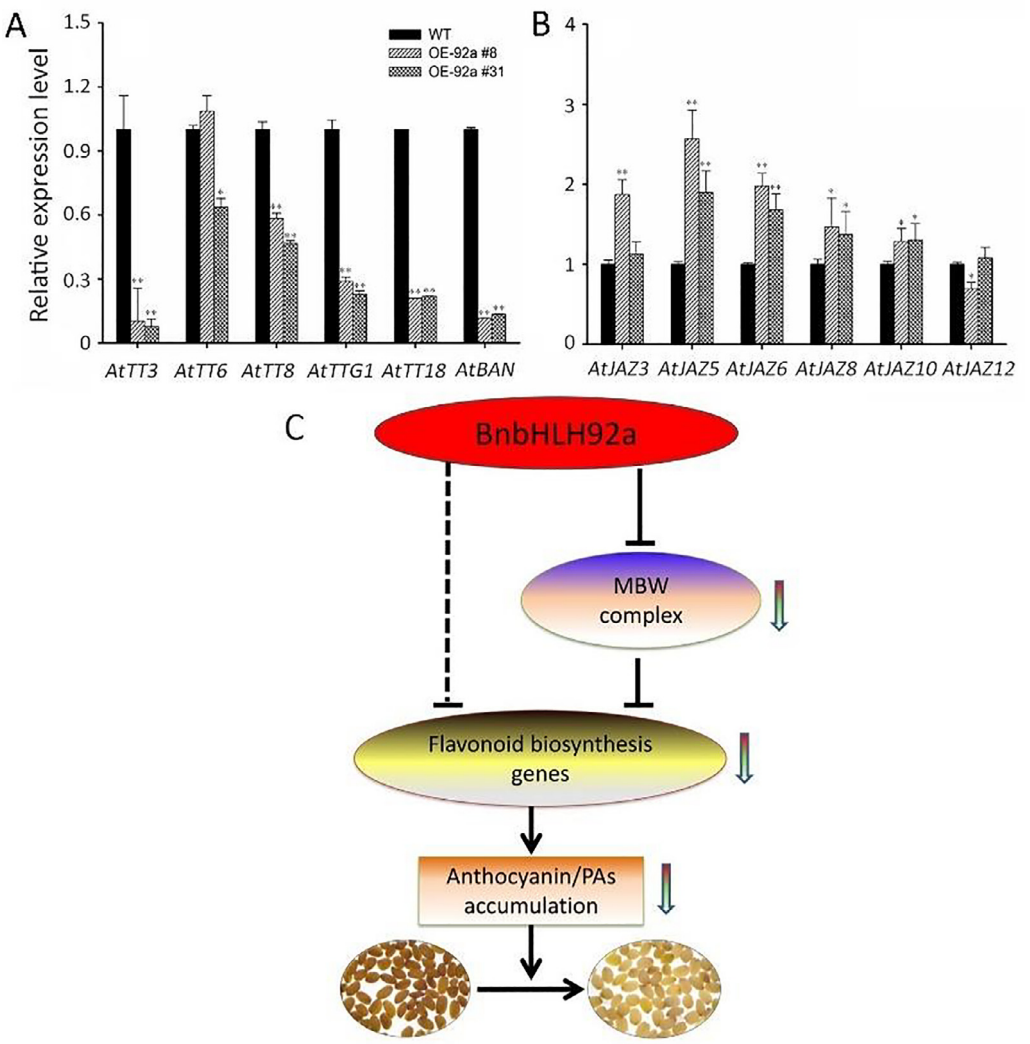

Fig. 4. The regulatory mechanism of *BnbHLH92a* in *Arabidopsis*. (A, B) Relative expression levels of flavonoid biosynthesis genes and *AtJAZ* genes in the wild-type and *OE-92a Arabidopsis* lines were detected by qRT-PCR. Values are mean ± SD of three biological replicates (*, $P < 0.05$; **, $P < 0.01$). (C) The potential regulatory network of BnbHLH92a in *OE-92a Arabidopsis* lines. Downward arrows indicate down-regulated gene expression or reduced metabolite content.

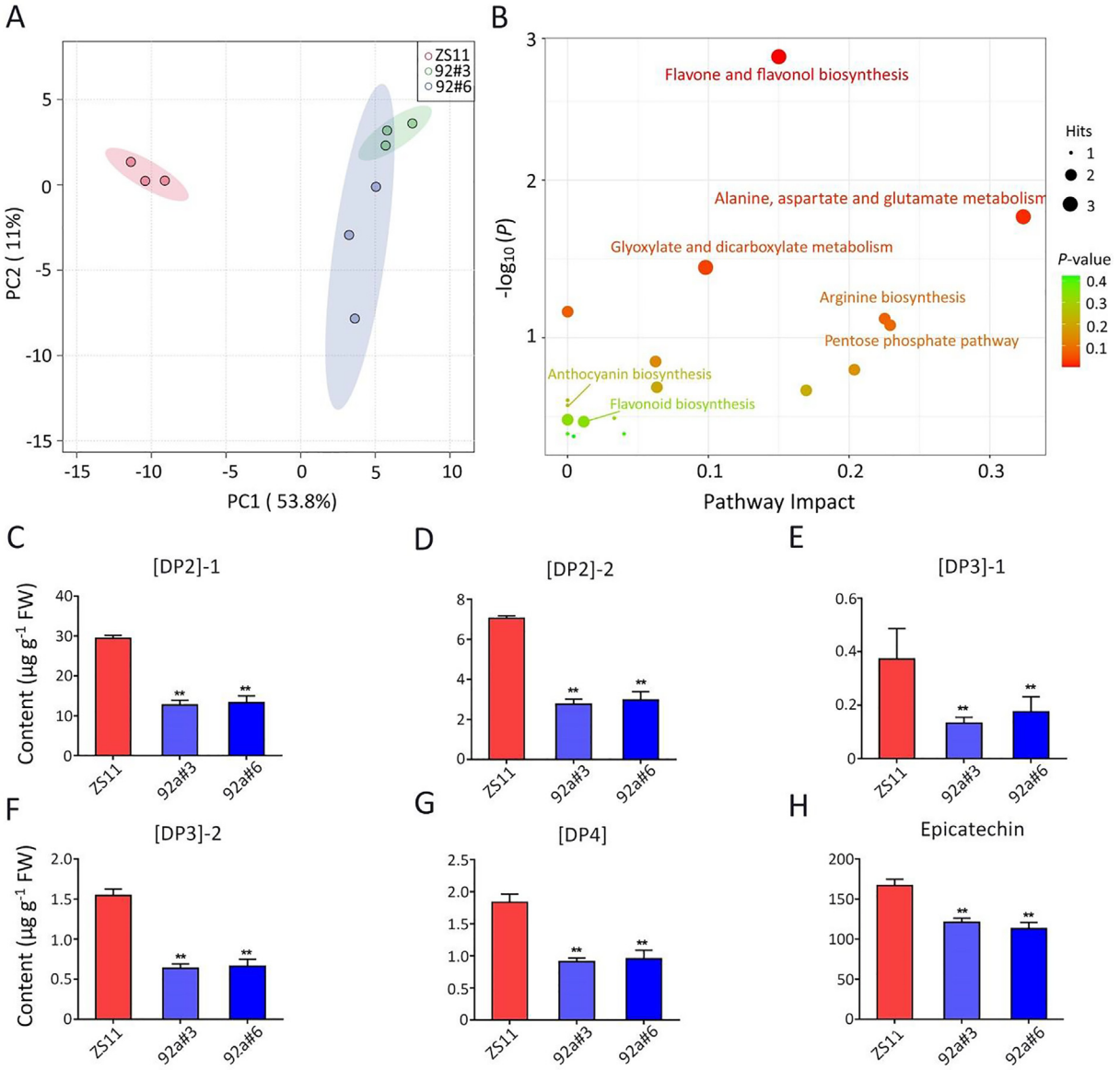

Fig. 5. Differentially abundant flavonoids identified by UPLC-HESI-MS/MS in seeds of ZS11 and *OE-BnbHLH92a B. napus* lines. (A) PCA score plot of metabolite profiles of ZS11 and *OE-BnbHLH92a* lines. (B) Enrichment analysis of differential metabolite KEGG. (C–H) Flavonoids with significantly different abundance identified by UPLC-HESI-MS/MS in seed extracts of ZS11 vs. *OE-BnbHLH92a B. napus.* Values are mean ± SD of three biological replicates (**, $P < 0.01$).

overexpression of *BnbHLH92a* inhibited the expression of *AtTT3*, *AtTT18*, *AtBAN*, *AtTT8*, *AtTTG1*, and *AtJAZ* genes (Fig. 4). To better understand the mechanism of BnbHLH92a's involvement in the flavonoid biosynthesis pathway in *B. napus*, we identified proteins potentially interacting with BnbHLH92a using yeast two-hybrid (Y2H) assays. We observed interaction between BnbHLH92a and BnTTG1 (Fig. 6A; Table S2), and further confirmed their interaction by bimolecular fluorescence complementation (BiFC) assays. First, we confirmed the subcellular localization of BnTTG1 in *N. benthamiana* epidermal cells: the control GFP signal was distributed throughout the entire cell, whereas the Pro35S:BnTTG1a-GFP fusion protein accumulated in both the nucleus and cytoplasm, and the Pro35S:BnTTG1b-GFP fusion protein was localized to the nucleus (Fig. 6B). These findings are consistent with the observation that TTG1 is localized to both the nucleus and cytoplasm in *A. thaliana* [65]. Second, we fused BnbHLH92a to the C-terminal half of yellow fluorescent protein (YFP), and BnTTG1a and BnTTG1b to the N-terminal half of YFP. In the BiFC assay, we detected yellow fluorescent signals in *N. benthamiana* epidermal cells co-transfected with plasmids that harbored either the cYFP–*BnbHLH92a* and nYFP–*BnTTG1a* fusion genes or the cYFP–*BnbHLH92a* and nYFP–*BnTTG1b* fusion genes (Fig. 6C, D). These signals showed that BnbHLH92a interacted physically with BnTTG1 *in vivo*.

3.6. BnbHLH92a directly binds to the BnTT18 promoter and suppresses its expression

Our findings indicated that BnbHLH92a was a negative regulator of flavonoid biosynthesis. Among the genes encoding enzymes involved in flavonoid biosynthesis, *TT3*, *TT18*, and *BAN* are late biosynthetic genes (LBGs) that are regulated by the MBW ternary complex of transcription factors (R2R3-MYB, bHLH, and WD40) [28,39]. To investigate this process in detail, we searched for BnbHLH92a-targeted genes using the *cis*-acting regulatory elements known as G boxes, which are bHLH-type transcription factor recognition sites [46,62]. We identified multiple *cis*-acting regulatory element G boxes in the *BnTT18* promoter regions (Fig. 7A;

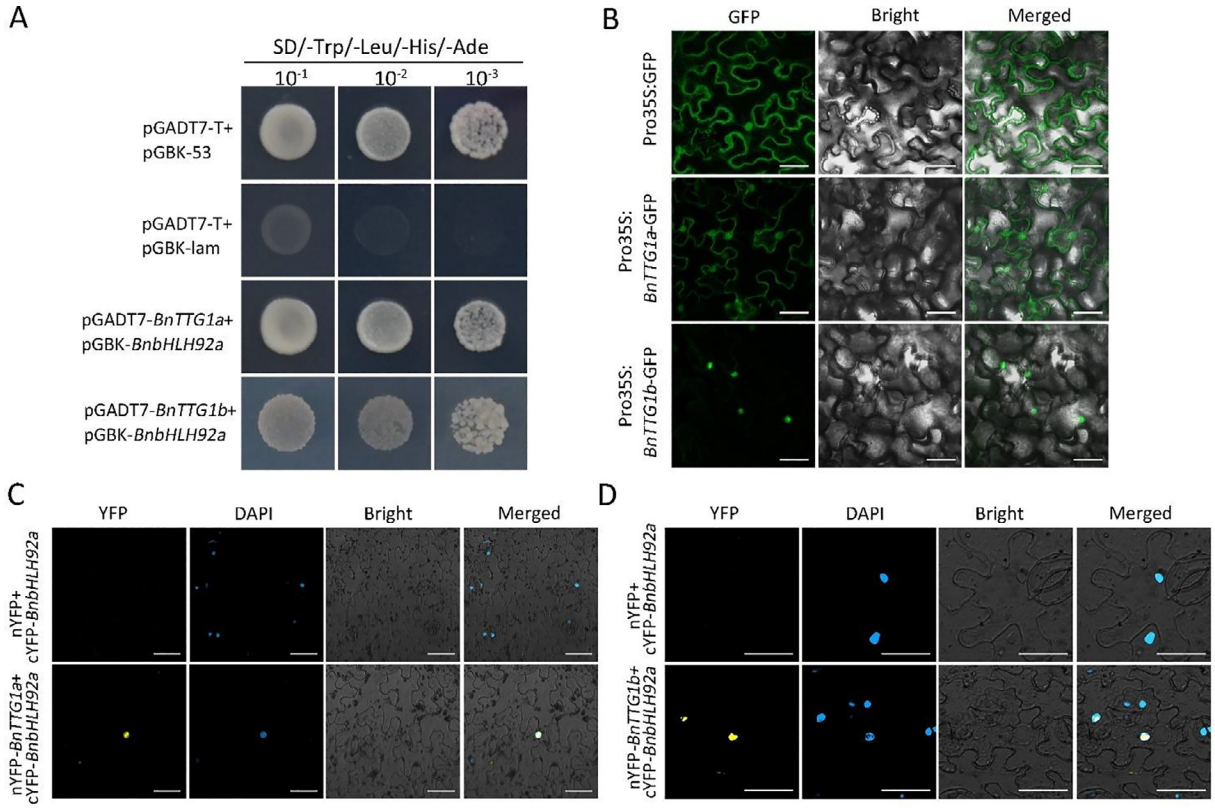

Fig. 6. BnbHLH92a interacts with BnTTG1. (A) Yeast two-hybrid assay of the interaction between BnbHLH92a and BnTTG1. Tenfold serial dilutions of transformed yeast cells were grown on SD-Trp/-Leu/-His/-Ade medium. (B) Subcellular localization of BnTTG1-GFP fusion proteins in *N. benthamiana* leaf epidermal cells. Bright-field images are compared. Scale bars, 50 μm. (C) BiFC analysis of the interaction between BnbHLH92a and BnTTG1a in *N. benthamiana* leaf epidermal cells. (D) BiFC analysis of the interaction between BnbHLH92a and BnTTG1b in *N. benthamiana* leaf epidermal cells. DAPI is a nuclear staining dye. Scale bars, 50 μm.

Table S2), suggesting that *BnTT18* may be directly regulated by BnbHLH92a. The dual-luciferase reporter plasmids used in these assays harbored the *BnTT18* promoter fused to LUC, and REN driven by the CaMV 35S promoter served as an internal control, while plasmids containing full-length *BnbHLH92a* cDNA were used as effectors (Fig. 7B). The activity of the *BnTT18* promoter was significantly reduced in the presence of BnbHLH92a (Fig. 7C).

We next employed ChIP analysis to further verify the direct binding of BnbHLH92a to the promoter region of *BnTT18* using chromatin isolated from seeds of transgenic rapeseed OE-BnbHLH92a and anti-GFP antibodies. According to the included G-box binding elements and the visible peak shape of the promoter region (Fig. 7A and D), primers for amplifying possible binding sites were designed. The ChIP-qPCR results showed that BnbHLH92a directly binds to the fragments of the *BnTT18* promoter, especially to the sites of F2 and F3 regions (Fig. 7E). Collectively, these results suggest that BnbHLH92a binds directly to the promoter of *BnTT18* to negatively regulate the flavonoid biosynthesis pathway in *B. napus*.

4. Discussion

In recent decades, the MBW (R2R3-MYB, bHLH, and WD40) ternary complexes governing the flavonoid biosynthesis pathway has been well studied in many species [28,39]. But little is known about anthocyanin or PA pathway targets of MBW regulatory model to regulate structural genes in rapeseed. Recently, *LcbHLH92* was found to act as a negative regulator of anthocyanin/proanthocyandin accumulation in sheepgrass [46]. In the present study, BnbHLH92a shared high identity with counterparts in *Arabidopsis* and *Lotus japonicus* (Fig. S3), suggesting a similar function of these transcription factors. We found that BnbHLH92a functions as a transcriptional repressor (Fig. 1). We previously demonstrated that polymeric phenolic compounds initially accumulate in the hilum of *B. napus* seeds, functioning in the formation of seed color [22]. The finding that *BnbHLH92a* is not only expressed specifically in the hilum, but also differs between yellow-seeded and black-seeded varieties with high expression in developing seed, seed coat, episperm, funicle, and silique pod (Fig. 1) suggests that BnbHLH92a acts in determining the color of the seed coat in *B. napus*. *BnbHLH92a* disruption of flavonoid biosynthesis in transgenic *Arabidopsis* resulted in a yellow-seeded phenotype (Figs. 2, S4). Quantitative analysis by UPLC-HESI-MS/MS confirmed that overexpressing *BnbHLH92a* in *A. thaliana* reduced the accumulation of primary phenolic and flavonoid components (Fig. S5; Table 1), in agreement with published findings [18,22] that epicatechin and proanthocyanidin metabolites are the main factors governing seed coat color in *Brassica* crops. The finding that flavonoid content decreased in *OE-BnbHLH92a* rapeseed lines compared to ZS11 (Fig. 5) is consistent with those in transgenic *Arabidopsis* plants (Fig. 3). The finding that the seed color and metabolites of PAs (epicatechin, [DP2]-1, [DP2]-2, [DP3]-1, [DP3]-2, and [DP4]) did not differ between mature seeds of the *AtbHLH92* mutant and WT in *Arabidopsis* (Fig. S6) indicates a much more complex molecular mechanism underlying anthocyanin and PA biosynthesis in rapeseed than in *Arabidopsis*. Our results reveal the potential role of *BnbHLH92a* in regulation of anthocyanin and PA biosynthesis in *B. napus*.

Genes of the general anthocyanin and PA pathway (*TT3*, *TT18*, and *BAN*), are regulated primarily by MBW ternary complexes (R2R3-MYB, bHLH, and WD40) [28,39], in particular the TT2-TT8-TTG1 complex [41,45,66]. In this study, the expression of *AtTT8*

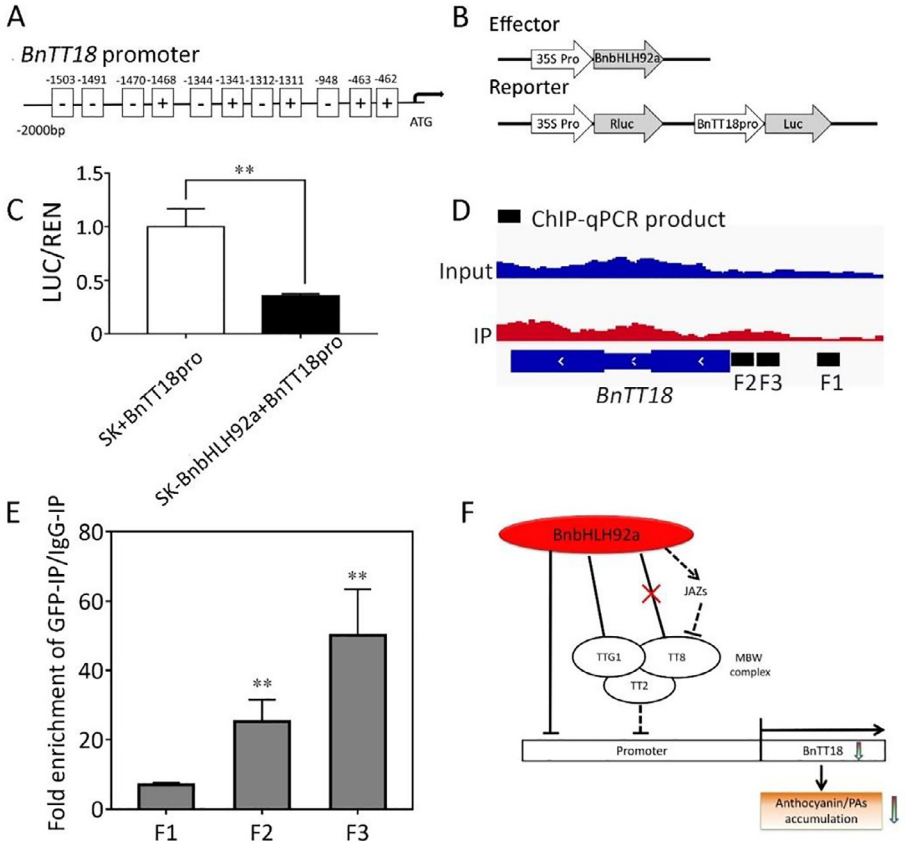

Fig. 7. The regulation mechanism of *BnbHLH92a* in *B. napus*. (A) Distribution of canonical and core G-box elements in the promoter region of *BnTT18*. (B) Schematic diagram of the double-reporter and effector plasmids used in the dual-luciferase assay. (C) Dual-luciferase reporter assays demonstrating that BnbHLH92a inhibits the activity of the *BnTT18* promoter. Values for blank effector were normalized to 1. SK, empty vector. Values are mean ± SD from three biological repeats (**, $P < 0.01$). (D) Peak pattern distribution of the target gene *BnTT18* promoter region. (E) Association of BnbHLH92a with its targets by ChIP-qPCR assay. Chromatin prepared OE-BnbHLH92a *B. napus* seed using anti-BnbHLH92a antibody (IP) were detected by qPCR with IgG as the control. Values are mean ± SD of three biological replicates (**, $P < 0.01$). (F) Proposed schematic model for the role of BnbHLH92a as a negative regulator that fine-tunes the biosynthesis of anthocyanins and PAs. TT2, TT8 and TTG1 form ternary MBW complexes, which affect anthocyanins and PAs by regulating the expression of late biosynthetic genes in the flavonoid pathway. Downward arrows indicate down-regulated gene expression or reduced metabolite content.

was inhibited, whereas the *AtJAZ* genes were all activated, by ectopic expression of *BnbHLH92a* in transgenic *Arabidopsis* (Fig. 4). These observations followed the findings [30,46,64] that anthocyanin and PA contents are reduced in plants with JAZ protein–mediated inhibition of *TT8* expression. We found that BnbHLH92a physically interacted with BnTTG1 (BnTTG1a and BnTTG1b), which may function alone or interact with other proteins to positively regulate anthocyanin production and seed coat pigmentation [28,66,67], and the expression of *AtTTG1* was inhibited in the *OE-92a* lines (Fig. 4). We accordingly propose that BnbHLH92a interacts with BnTTG1 as a novel complex for negatively regulating anthocyanin and PA accumulation in rapeseed. The dual-luciferase assay, ChIP and qPCR analysis (Fig. 7) revealed that BnbHLH92a directly binds to the promoter region of *BnTT18*, suppressing the accumulation of PAs in transgenic plants. These findings suggest that a negative feedback mechanism involving *BnbHLH92a* might represent a gene regulatory network for anthocyanin and PA biosynthesis during seed development in *B. napus*.

This work not only showed the role of BnbHLH92a as a negative regulator of the anthocyanin and PA biosynthesis pathway, but also provided molecular evidence that BnbHLH92a directly interacts with BnTTG1 and binds the promoter of *BnTT18*, resulting in reduced anthocyanin and PA accumulation in *B. napus*. Based on these findings, we propose a model (Fig. 7F) for the role of BnbHLH92a in regulating the anthocyanin and PA biosynthesis pathway. Our results lay a foundation for elucidating the mechanisms regulating biosynthesis of anthocyanins and PAs and will be useful for designing strategies for the genetic improvement of *B. napus*.

CRediT authorship contribution statement

Ran Hu: Conceptualization, Data curation, Formal analysis, Investigation, Methodology, Software, Validation, Visualization, Writing-original draft, Writing-review & editing. **Meichen Zhu:** Data curation, Formal analysis, Investigation, Methodology. **Si Chen:** Investigation, Methodology. **Chengxiang Li:** Writing-original draft, Writing-review & editing. **Qianwei Zhang:** Investigation, Methodology. **Lei Gao:** Resources, Validation. **Xueqin Liu:** Resources, Validation. **Shulin Shen:** Software, Resources. **Fuyou Fu:** Methodology. **Xinfu Xu:** Resources. **Ying Liang:** Resources. **Liezhao Liu:** Resources. **Kun Lu:** Software, Resources. **Hao Yu:** Writing-Review & Editing. **Jiana Li:** Funding Acquisition, Project Administration, Supervision, Writing-original draft, Writing-review & editing. **Cunmin Qu:** Conceptualization, Funding Acquisition, Project Administration, Supervision, Writing-original draft, Writing-review & editing.

Declaration of competing interest

The authors declare that they have no known competing financial interests or personal relationships that could have appeared to influence the work reported in this paper.

Acknowledgments

This work was supported by the National Natural Science Foundation of China (32072093, 31830067), the China Agriculture Research System of MOF and MARA, the Science and Enterprise Consortium Project of Chongqing (cqnyncw-kqlhtxm), the Innovation and Entrepreneurship Training Program for Undergraduates (S202010635197), and the 111 Project (B12006). The authors thank Yan Zhou for her assistance with our experiments, and Dr. Pu Yan (Institute of Tropical Bioscience and Biotechnology, Chinese Academy of Tropical Agricultural Sciences, Haikou, Hainan, China) for providing nimble cloning vectors and technical advice.

Appendix A. Supplementary data

Supplementary data for this article can be found online at https://doi.org/10.1016/j.cj.2022.07.015.

References

[1] Q. Hu, W. Hua, Y. Yin, X. Zhang, L. Liu, J. Shi, Y. Zhao, L.U. Qin, C. Chen, H. Wang, Rapeseed research and production in China, Crop J. 5 (2017) 127–135.
[2] M.H. Rahman, M. Joersbo, M.H. Poulsen, Development of yellow-seeded *Brassica napus* of double low quality, Plant Breed. 120 (2001) 473–478.
[3] B.Y. Chen, W.K. Heneen, R. Jönsson, Resynthesis of *Brassies napus* L. through interspecific hybridization between *B. alboglabra* Bailey and *B. campestris* L. with special emphasis on seed color, Plant Breed. 101 (1988) 52–59.
[4] A. Rashid, G. Rakow, R.K. Downey, Development of yellow seeded *Brassica napus* through interspecific crosses, Plant Breed. 112 (1994) 127–134.
[5] A. Li, J. Jiang, Y. Zhang, R.J. Snowdon, G. Liang, Y. Wang, Molecular and cytological characterization of introgression lines in yellow seed derived from somatic hybrids between *Brassica napus* and *Sinapis alba*, Mol. Breed. 29 (2012) 209–219.
[6] J. Wen, L. Zhu, L. Qi, H. Ke, B. Yi, J. Shen, J. Tu, C. Ma, T.D. Fu, Characterization of interploid hybrids from crosses between *Brassica juncea* and *B. oleracea* and the production of yellow-seeded *B. napus*, Theor. Appl. Genet. 125 (2012) 19–32.
[7] Z.W. Liu, T.D. Fu, J.X. Tu, B.Y. Chen, Inheritance of seed color and identification of RAPD and AFLP markers linked to the seed color gene in rapeseed (*Brassica napus* L.), Theor. Appl. Genet. 110 (2005) 303–310.
[8] J.P. Gustafson, A.G. Badani, R.J. Snowdon, B. Wittkop, F.D. Lipsa, R. Baetzel, R. Horn, A.D. Haro, R. Font, W. Lühs, W. Friedt, Colocalization of a partially dominant gene for yellow seed colour with a major QTL influencing acid detergent fibre ADF) content in different crosses of oilseed rape *Brassica napus*, Genome 49 (2006) 1499–1509.
[9] A.E.V. Deynze, W.D. Beversdorf, K.P. Pauls, Temperature effects on seed color in black- and yellow-seeded rapeseed, Can. J. Plant Sci. 73 (1993) 383–387.
[10] MA.S. Marles, M.Y. Gruber, Histochemical characterisation of unextractable seed coat pigments and quantification of extractable lignin in the Brassicaceae, J. Sci. Food Agric. 84 (2004) 251–262.
[11] L. Akhov, P. Ashe, Y.F. Tang, R. Datla, G. Selvaraj, Proanthocyanidin biosynthesis in the seed coat of yellow-seeded, canola quality *Brassica napus* YN01-429 is constrained at the committed step catalyzed by dihydroflavonol 4-reductase, Botany 87 (2009) 616–625.
[12] N. Nesi, M.O. Lucas, B. Auger, C. Baron, A. Lécureuil, P. Guerche, J. Kronenberger, L. Lepiniec, I. Debeaujon, M. Renard, The promoter of the *Arabidopsis thaliana BAN* gene is active in tannin-accumulating cells of the *Brassica napus* seed coat, Plant Cell Rep. 28 (2009) 601–617.
[13] F. He, Q.H. Pan, Y. Shi, C.Q. Duan, Biosynthesis and genetic regulation of proanthocyanidins in plants, Molecules 13 (2008) 2674–2703.
[14] A. Baudry, M.A. Heim, B. Dubreucq, M. Caboche, B. Weisshaar, L. Lepiniec, TT2, TT8, and TTG1 synergistically specify the expression of *BANYULS* and proanthocyanidin biosynthesis in *Arabidopsis thaliana*, Plant J. 39 (2004) 366–380.
[15] L. Lepiniec, I. Debeaujon, J.M. Routaboul, A. Baudry, L. Pourcel, N. Nesi, M. Caboche, Genetics and biochemistry of seed flavonoids, Annu. Rev. Plant Biol. 57 (2006) 405–430.
[16] L.L. Wan, Q. Xia, X. Qiu, G. Selvaraj, Early stages of seed development in *Brassica napus*: a seed coat-specific cysteine proteinase associated with programmed cell death of the inner integument, Plant J. 30 (2002) 1–10.
[17] J. Zhang, Y. Lu, Y. Yuan, X. Zhang, J. Geng, Y.U. Chen, S. Cloutier, P.B.E. McVetty, G. Li, Map-based cloning and characterization of a gene controlling hairiness and seed coat color traits in *Brassica rapa*, Plant Mol. Biol. 69 (2009) 553–563.
[18] X. Li, L.I. Chen, M. Hong, Y. Zhang, F. Zu, J. Wen, B. Yi, C. Ma, J. Shen, J. Tu, T. Fu, J. Schiefelbein, A large insertion in bHLH transcription factor *BrTT8* resulting in yellow seed coat in *Brassica rapa*, PLoS ONE 7 (2012) e44145.
[19] L.K. Padmaja, P. Agarwal, V. Gupta, A. Mukhopadhyay, Y.S. Sodhi, D. Pental, A.K. Pradhan, Natural mutations in two homoeologous *TT8* genes control yellow seed coat trait in allotetraploid *Brassica juncea* (AABB), Theor. Appl. Genet. 127 (2014) 339–347.
[20] Y. Zhai, K. Yu, S. Cai, L. Hu, O. Amoo, L. Xu, Y. Yang, B. Ma, Y. Jiao, C. Zhang, M.H. U. Khan, S.U. Khan, C. Fan, Y. Zhou, Targeted mutagenesis of *BnTT8* homologs controls yellow seed coat development for effective oil production in *Brassica napus* L., Plant Biotechnol. J. 18 (2020) 1153–1168.
[21] J.P. Lian, X.C. Lu, N.W. Yin, L.J. Ma, J. Lu, X. Liu, J.N. Li, J. Lu, B. Lei, R. Wang, Y.R. Chai, Silencing of BnTT1 family genes affects seed flavonoid biosynthesis and alters seed fatty acid composition in *Brassica napus*, Plant Sci. 254 (2017) 32–47.
[22] C.M. Qu, F.Y. Fu, K. Lu, K. Zhang, R. Wang, X.F. Xu, M. Wang, J.X. Lu, H.F. Wan, Z. L. Tang, J.N. Li, Differential accumulation of phenolic compounds and expression of related genes in black-and yellow-seeded *Brassica napus*, J. Exp. Bot. 64 (2013) 2885–2898.
[23] T. Saigo, T. Wang, M. Watanabe, T. Tohge, Diversity of anthocyanin and proanthocyanin biosynthesis in land plants, Curr. Opin. Plant Biol. 55 (2020) 93–99.
[24] D.W. Zhang, L.l. Liu, D.G. Zhou, X.J. Liu, Z.S. Liu, M.l. Yan, Genome-wide identification and expression analysis of anthocyanin biosynthetic genes in *Brassica juncea*, J. Integr. Agric. 19 (2020) 1250–1260.
[25] Y.Y. Zhang, G.J. Wang, L.X. Li, Y.H. Li, B. Zhou, H.F. Yan, Identification and expression analysis of BrTT8 during anthocyanin biosynthesis and exposure to abiotic stress in turnip (*Brassica rapa* subsp. rapa 'Tsuda'), Sci. Hortic. 268 (2020) 109332.
[26] S.C. Zou, J.C. Wu, M.Q. Shahid, Y. He, S.Q. Lin, Z.H. Liu, X.H. Yang, Identification of key taste components in loquat using widely targeted metabolomics, Food Chem. 323 (2020) 126822.
[27] I. Hichri, F. Barrieu, J. Bogs, C. Kappel, S. Delrot, V. Lauvergeat, Recent advances in the transcriptional regulation of the flavonoid biosynthetic pathway, J. Exp. Bot. 62 (2011) 2465–2483.
[28] W. Xu, C. Dubos, L. Lepiniec, Transcriptional control of flavonoid biosynthesis by MYB-bHLH-WDR complexes, Trends Plant Sci. 20 (2015) 176–185.
[29] S. Colanero, P. Perata, S. Gonzali, The *atroviolacea* gene encodes an R3-MYB protein repressing anthocyanin synthesis in tomato plants, Front. Plant Sci. 9 (2018) 830.
[30] W.J. Xu, D. Grain, S. Bobet, J.L. Gourrierec, J. Thévenin, Z. Kelemen, L. Lepiniec, C. Dubos, Complexity and robustness of the flavonoid transcriptional regulatory network revealed by comprehensive analyses of MYB-bHLH-WDR complexes and their targets in *Arabidopsis* seed, New Phytol. 202 (2014) 132–144.
[31] F. Gil-Muñoz, J.A. Sánchez-Navarro, C. Besada, A. Salvador, M.L. Badenes, M.D. M. Naval, G. Ríos, MBW complexes impinge on anthocyanidin reductase gene regulation for proanthocyanidin biosynthesis in persimmon fruit, Sci. Rep. 10 (2020) 3543.
[32] N.W. Albert, K.M. Davies, D.H. Lewis, H. Zhang, M. Montefiori, C. Brendolise, M. R. Boase, H. Ngo, P.E. Jameson, K.E. Schwinn, A conserved network of transcriptional activators and repressors regulates anthocyanin pigmentation in eudicots, Plant Cell 26 (2014) 962–980.
[33] E. Farcy, A. Cornu, Isolation and characterization of anthocyanin variants originating from the unstable system *an2-1* in *Petunia hybrida* (Hort.), Theor. Appl. Genet. 55 (1979) 273–278.
[34] C. Spelt, F. Quattrocchio, J.N.M. Mol, R. Koes, *anthocyanin1* of Petunia encodes a basic Helix-Loop-Helix protein that directly activates transcription of structural anthocyanin genes, Plant Cell 12 (2000) 1619–1631.
[35] H. Li, Z. Yang, Q.W. Zeng, S.B. Wang, Y.W. Luo, Y. Huang, Y.C. Xin, N.J. He, Abnormal expression of *bHLH3* disrupts a flavonoid homeostasis network, causing differences in pigment composition among mulberry fruits, Hort. Res. 7 (2020) 83.
[36] R. Zhao, X. Song, N. Yang, L. Chen, L. Xiang, X.Q. Liu, K. Zhao, Expression of the subgroup IIIf bHLH transcription factor CpbHLH1 from *Chimonanthus praecox* (L.) in transgenic model plants inhibits anthocyanin accumulation, Plant Cell Rep. 39 (2020) 891–907.
[37] F. Mehrtens, H. Kranz, P. Bednarek, B. Weisshaar, The *Arabidopsis* transcription factor MYB12 is a flavonol-specific regulator of phenylpropanoid biosynthesis, Plant Physiol. 138 (2005) 1083–1096.
[38] X.W. Qi, H.L. Fang, Z.Q. Chen, Z.Q. Liu, X. Yu, C.Y. Liang, Ectopic expression of a R2R3-MYB transcription factor gene *LjaMYB12* from *Lonicera japonica* increases flavonoid accumulation in *Arabidopsis thaliana*, Int. J. Mol. Sci. 20 (2019) 4494.
[39] R. Stracke, H. Ishihara, G. Huep, A. Barsch, F. Mehrtens, K. Niehaus, B. Weisshaar, Differential regulation of closely related R2R3-MYB transcription factors controls flavonol accumulation in different parts of the *Arabidopsis thaliana* seedling, Plant J. 50 (2007) 660–677.
[40] M. Zhao, J.M. Leavitt, A.M. Lloyd, Regulation of the anthocyanin biosynthetic pathway by the TTG1/bHLH/Myb transcriptional complex in *Arabidopsis* seedlings, Plant J. 53 (2008) 814–827.
[41] N. Nesi, I. Debeaujon, C. Jond, G. Pelletier, M. Caboche, L. Lepiniec, The *TT8* gene encodes a basic Helix-Loop-Helix domain protein required for expression of *DFR* and *BAN* genes in *Arabidopsis* siliques, Plant Cell 12 (2000) 1863–1878.
[42] H. Xu, N. Wang, J. Liu, C. Qu, Y. Wang, S. Jiang, N. Lu, D. Wang, Z. Zhang, X. Chen, The molecular mechanism underlying anthocyanin metabolism in apple using the *MdMYB16* and *MdbHLH33* genes, Plant Mol. Biol. 94 (2017) 149–165.
[43] L.F. Yao, B. Yang, B.S. Xian, B.S. Chen, J.G. Yan, Q.Q. Chen, S.D. Gao, P.Y. Zhao, F. Han, J.W. Xu, Y.Q. Jiang, The R2R3-MYB transcription factor BnaMYB111L from rapeseed modulates reactive oxygen species accumulation and hypersensitive-like cell death, Plant Physiol. Biochem. 147 (2020) 280–288.
[44] L.H. Wang, W. Tang, Y. Hu, Y.B. Zhang, J.Q. Sun, X.H. Guo, H. Lu, Y. Yang, C.B. Fang, X.L. Niu, J.Y. Yue, Z.J. Fei, Y.S. Liu, A MYB/bHLH complex regulates tissue-

specific anthocyanin biosynthesis in the inner pericarp of red-centered kiwifruit *Actinidia chinensis* cv, Hongyang, Plant J. 99 (2019) 359–378.
[45] N. Nesi, C. Jond, I. Debeaujon, M. Caboche, L. Lepiniec, The *Arabidopsis TT2* gene encodes an R2R3 MYB domain protein that acts as a key determinant for proanthocyanidin accumulation in developing seed, Plant Cell 13 (2001) 2099–2114.
[46] P.C. Zhao, X.X. Li, J.T. Jia, G.X. Yuan, S.Y. Chen, D.M. Qi, L.Q. Cheng, G.S. Liu, *bHLH92* from sheepgrass acts as a negative regulator of anthocyanin/proanthocyandin accumulation and influences seed dormancy, J. Exp. Bot. 70 (2019) 269–284.
[47] M. Li, L. Sun, H. Gu, D.W. Cheng, X.Z. Guo, R. Chen, Z.Y. Wu, J.F. Jiang, X.C. Fan, J. Y. Chen, Genome-wide characterization and analysis of bHLH transcription factors related to anthocyanin biosynthesis in spine grapes (*Vitis davidii*), Sci. Rep. 11 (2021) 6863.
[48] S. Kumar, G. Stecher, K. Tamura, MEGA7: Molecular evolutionary genetics analysis version 7.0 for bigger datasets, Mol. Biol. Evol. 33 (2016) 1870–1874.
[49] H.Y. Chao, T. Li, C.Y. Luo, H.L. Huang, Y.F. Ruan, X.D. Li, Y. Niu, Y.H. Fan, W. Sun, K. Zhang, J.N. Li, C.M. Qu, K. Lu, BrassicaEDB: a gene expression database for *Brassica* crops, Int. J. Mol. Sci. 21 (2020) 5831.
[50] K.J. Livak, T.D. Schmittgen, Analysis of relative gene expression data using real-time quantitative PCR and the 2(-Delta Delta C(T)) Method, Methods 25 (2001) 402–408.
[51] K.W. Earley, J.R. Haag, O. Pontes, K. Opper, T. Juehne, K. Song, C.S. Pikaard, Gateway-compatible vectors for plant functional genomics and proteomics, Plant J. 45 (2006) 616–629.
[52] S.J. Clough, A.F. Bent, Floral dip: a simplified method for *Agrobacterium*-mediated transformation of *Arabidopsis thaliana*, Plant J. 16 (1998) 735–743.
[53] Y. Yang, K. Zhu, H. Li, S. Han, Q. Meng, S.U. Khan, C. Fan, K. Xie, Y. Zhou, Precise editing of CLAVATA genes in *Brassica napus* L. regulates multilocular silique development, Plant Biotechnol. J. 16 (2018) 1322–1335.
[54] P. Yan, Y.J. Zeng, W.T. Shen, D.C. Tuo, X.Y. Li, P. Zhou, Nimble Cloning: A simple, versatile, and efficient system for standardized molecular cloning, Front. Bioeng. Biotechnol. 15 (2020) 460.
[55] C. Li, S.M. Hu, Q.D. Lei, C.D. Wang, Y.Q. Yang, Y.P. Yang, X.D. Sun, Establishment and optimization of mRNA in situ hybridization system in turnip (*Brassica rapa* var. *rapa*), Plant Methods 15 (2019) 115.
[56] B. Niu, H. Deng, T. Li, S. Sharma, Q. Yun, Q. Li, Z. E, C. Chen, OsbZIP76 interacts with OsNF-YBs and regulates endosperm cellularization in rice (*Oryza sativa*), J. Integr. Plant Biol. 62 (2020) 1983–1996.
[57] S. Abraham, G.J. Tanner, P.J. Larkin, A.R. Ashton, Identification and biochemical characterization of mutants in the proanthocyanidin pathway in *Arabidopsis*, Plant Physiol. 130 (2002) 561–576.
[58] N. Li, H. Wu, Q. Ding, H. Li, Z. Li, J. Ding, Y.I. Li, The heterologous expression of *Arabidopsis* PAP2 induces anthocyanin accumulation and inhibits plant growth in tomato, Funct. Integr. Genomics 18 (2018) 341–353.
[59] M.X. Liang, E. Davis, D. Gardner, X.N. Cai, Y.J. Wu, Involvement of *AtLAC15* in lignin synthesis in seeds and in root elongation of *Arabidopsis*, Planta 224 (2006) 1185.
[60] J.M. Routaboul, L. Kerhoas, I. Debeaujon, L. Pourcel, M. Caboche, J. Einhorn, L. Lepiniec, Flavonoid diversity and biosynthesis in seed of *Arabidopsis thaliana*, Planta 224 (2006) 96–107.
[61] C. Qu, N. Yin, S.I. Chen, S. Wang, X. Chen, H. Zhao, S. Shen, F. Fu, B. Zhou, X. Xu, L. Liu, K. Lu, J. Li, Comparative analysis of the metabolic profiles of yellow- versus black-seeded rapeseed using UPLC-HESI-MS/MS and transcriptome analysis, J. Agric. Food Chem. 68 (2020) 3033–3049.
[62] Y.Z. Ke, Y.W. Wu, H.J. Zhou, P. Chen, M.M. Wang, M.M. Liu, P.F. Li, J. Yang, J.N. Li, H. Du, Genome-wide survey of the bHLH super gene family in *Brassica napus*, BMC Plant Biol. 20 (2020) 115.
[63] C. Mizzotti, I. Ezquer, D. Paolo, P. Rueda-Romero, R.F. Guerra, R. Battaglia, I. Rogachev, A. Aharoni, M.M. Kater, E. Caporali, L. Colombo, R.G. Franks, SEEDSTICK is a master regulator of development and metabolism in the *Arabidopsis* seed coat, PLoS Genet. 10 (2014) e1004856.
[64] T.C. Qi, S.S. Song, Q.C. Ren, D.W. Wu, H. Huang, Y. Chen, M. Fan, W. Peng, C.M. Ren, D.X. Xie, The Jasmonate-ZIM-domain proteins interact with the WD-Repeat/bHLH/MYB complexes to regulate Jasmonate-mediated anthocyanin accumulation and trichome initiation in *Arabidopsis thaliana*, Plant Cell 23 (2011) 1795–1814.
[65] C.X. Li, B. Zhang, B. Chen, L.H. Ji, H. Yu, Site-specific phosphorylation of TRANSPARENT TESTA GLABRA1 mediates carbon partitioning in *Arabidopsis* seeds, Nat. Commun. 9 (2018) 571.
[66] N.A. Ramsay, B.J. Glover, MYB–bHLH–WD40 protein complex and the evolution of cellular diversity, Trends Plant Sci. 10 (2005) 63–70.
[67] C.A. Airoldi, T.J. Hearn, S.F. Brockington, A.A.R. Webb, B.J. Glover, TTG1 proteins regulate circadian activity as well as epidermal cell fate and pigmentation, Nat. Plants 5 (2019) 1145–1153.